Journal of the Indian Society of Remote Sensing
https://doi.org/10.1007/s12524-021-01328-3

RESEARCH ARTICLE

Assessment of WRF-CHEM Simulated Dust Using Reanalysis, Satellite Data and Ground-Based Observations

Akshay Rajeev[1,2] · Charu Singh[1] · Sanjeev Kumar Singh[1] · Prakash Chauhan[1]

Received: 24 October 2020 / Accepted: 2 February 2021

Abstract
One of the significant natural pollutants in the atmosphere is the mineral dust aerosols. In the northern hemisphere, Arabian Peninsula is one of the significant sources of dust aerosols with the frequency of dust storms changing seasonally. Dust emitted from the Arabian Peninsula region transports towards the Indian region through prevailing winds, therefore a positive correlation between the extreme dust episodes over the Arabian region and air quality over the Indian region is generally observed. Therefore, there is a need to monitor and forecast such an episodic event over the Arabian Peninsula and surrounding regions so that substantial measures may be taken in Indian subcontinent to mitigate the adverse impact of low air quality on human being and several other sectors such as aviation, energy and infrastructure. In the present study, the WRF-Chem simulations for dust particles are assessed against the observational data sets (i.e. MERRA-2, MODIS-Terra, Aura-OMI, CPCB). Based on the comparison of WRF-Chem simulated data sets with the satellite/reanalysis data, it is noted that in the post-monsoon season, WRF-Chem model can capture the entire dust episode (emission, transportation and dissipation) reasonably well. From the statistical analysis (PDF, CDF, Scatter plot and Temporal evolution), it was noted that there was a consistent underestimation of the simulated dust by WRF-Chem as compared to the observational data sets. A statistically robust categorical analysis has also been carried out for assessing the performance of WRF-Chem with respect to the observations for each dust event, and it is noted that on an average the probability of detection of dust event is about 77% and false alarm ratio is about 15% with an overall accuracy of 76%. Results obtained from the present analysis are encouraging and would be useful for the assessment of WRF-Chem simulations for other seasons also.

Keywords Dust · Arabian peninsula · Air quality · WRF-CHEM · Probability of detection

Introduction

Aerosols present in the atmosphere can be from a natural source or an anthropogenic source. Natural aerosols are primarily sea salt and mineral dust. Dust or mineral dust is minute soil particles that are suspended in the atmosphere. They originate primarily from arid and semi-arid regions with deficient annual rainfall (Ginoux et al. 2004, 2012; Goudie and Middleton 2006) and wind speeds (Shao 2009) greater than 10 m/sec. They undergo both regional to intercontinental transportation. In the northern hemisphere, the primary dust sources are Sahara and Sahel in North Africa, Wahiba sands area of Oman in the Middle East and Southwest and East Asia. These natural sources are mainly located in the arid and semi-arid regions, which includes deserts, dry lake beds and temporary river beds. The anthropogenic sources include those due to construction, human-induced droughts and agricultural practices. An increase in atmospheric dust load has also been observed as a consequence of an increase in anthropogenic activities (Prospero et al. 2002; Tegen and Fung 1994). The most considerable contribution of dust aerosols to the

✉ Charu Singh
charu@iirs.gov.in

Akshay Rajeev
rajeev_akshay@iitgn.ac.in

Sanjeev Kumar Singh
sksingh@iirs.gov.in

Prakash Chauhan
director@iirs.gov.in

[1] Indian Institute of Remote Sensing, ISRO, Dehradun, Uttarakhand, India

[2] Present Address: IIT Gandhinagar, Gujarat, India

Published online: 05 March 2021

atmosphere is from the Northern Hemisphere owing to a more significant proportion of land coverage. The Sahara desert is the single largest source of dust on the planet with an estimated global emission of 670 Mt/yr (Rajot et al. 2008). The major factors which contribute to the higher dust load values over this region are the larger area over which dust is lifted and the strong winds (Su and Toon 2011). Observations and simulations show a seasonal change in the wind speed, and the dry condition has also contributed to significant variation in the concentration of dust in the atmosphere (Gong et al. 2012; Kaufman et al. 2005). Currently, it is understood that the highest and maximum dust load events occur during the summer seasons. Such observations were made in the Sahara and Arabian Peninsula as well as in various other parts of the northern hemisphere where the frequency of dust load events is higher during June, July and August (Goudie and Middleton 2006).

Dust aerosols severely degrade air quality and are also harmful to organisms (Iii et al. 2002; Pease et al. 1998; Prospero 1999). The dust acts as a source of nutrients for remote oceans which influence the marine biogeochemical cycles, which in turn affect the carbon uptake by oceans (Andreae et al. 1986; Jickells et al. 2005). They directly impact the climate by absorbing and scattering incoming solar radiation (Choobari et al. 2014; Hansell et al. 2010; McCormick and Ludwig 1967; Miller and Tegen 1998; Miller et al. 2004). They affect the climate semi-directly by changing the temperature structure of the atmosphere and cloud-burning effect (Ackerman et al. 2000; Hansen et al. 1997; Koren et al. 2004). The climate is indirectly influenced by the dust aerosols due to the effects of the dust on the optical properties of clouds and on the pattern of precipitation formation (Gunn and Phillips 1957; Jing Su et al. 2008; Liou and Ou 1989). Studies have demonstrated that the cloud cooling effect has been substantially reduced at the surface and TOA by the dust aerosols (Santos et al. 2013). Present values of the radiative forcing by dust have many significant uncertainties (Dubovik et al. 2002; Durant et al. 2009). These uncertainties arise because of uncertainties in estimates of global dust load (Dubovik et al. 2002; Ginoux et al. 2012; McGowan and Soderholm 2012) and also as a result of the complex physical and chemical properties of dust aerosols and its relation with the radiation budget (Science 2020; Sokolik et al. 2001). Several studies have also shown the dust aerosols substantially affect the India summer monsoon variability (Jin et al. 2014, 2015; Singh et al. 2017 a, b, 2018, 2019a, b; Vinoj et al. 2014).

Dust aerosols can be transported over distances ranging from intercontinental to regional scale (Dey et al. 2004; Engelstaedter et al. 2006; Griffinet al. 2002; Uno et al. 2009). The activity of dust during the summer is mainly controlled by the strong seasonal cycle. Observations show that dust storms are more frequent over the Arabian Peninsula, Iraq, Iran, Jordan, Lebanon, Syria and southern Egypt during the spring (Middleton 1986; Orlovsky et al. 2005). In contrast, in northern Egypt, the frequency of dust storms is higher in the winter. The transport path of the dust aerosols also changes seasonally. Its location strongly influences their residence time in the atmosphere, its size and the type of process taking place there (Wang et al. 2013). Observations by (Bolin et al. 1974) show that the particles in the upper troposphere have a longer lifetime compared to those in the lower troposphere. They found that the dust particles with relatively larger size fall out rapidly near the source because of the gravitational effect whereas the smaller particles remain suspended for extended periods.

In recent years, attempts have been made to analyse and monitor the extreme dust episodes using numerical models (Alonso-Pérez et al. 2012; Cavazos-Guerra and Todd 2012; Dumka et al. 2019; Kedia et al. 2018; Kumar et al. 2014; Singh et al. 2020; Ukhov et al. 2020) owing to wide spread impact of such activities on social and economy sectors. However, model simulated output may not exactly resolve atmospheric processes due to various reasons such as complexities involve in simulating the nonlinear processes, model physics and dust emission mechanism (Nabavi et al. 2017; Lin Su and Fung 2015; Zeng et al. 2017), therefore it is essential to analyse model simulated output with respect to the observational, remote sensing data sets. In the present study, an attempt has been made to evaluate Weather Research and Forecasting coupled with Chemistry (WRF-Chem) generated forecast of dust aerosols against observational data sets using various statistical measures.

Materials and Methods

Study Area

The region under investigation in this work is shown in Fig. 1. The areal extent of this study area is between 5° N to 38° N and 50° E to 98° E which includes some of the significant dust sources in the Northern Hemisphere such as Afghanistan, Arabian Peninsula, Iran, India and Pakistan. The particular study area was chosen to understand the formation of dust storms over these source regions and its effects on the air quality over the Indian subcontinent.

Fig. 1 Area of study

Dataset

WRF-Chem Simulated Output

Two days forecasting is being generated using WRF-Chem at IIRS. For more details of the dataset, IIRS air quality portal (https://airquality.iirs.gov.in) may be referred. The dataset is available at 0.25° X 0.25° resolution for every 6 h. The variables considered for this study are Dust load (g/m2), PM10 and PM2.5. WRF-Chem model output is assessed based on various observational and reanalysis datasets.

A variant of the numerical prediction model WRF has been used for the simulation of the dust episodes. WRF model is an advanced mesoscale forecast model that is mainly instrumental for understanding and predicting weather phenomenon. WRF can be employed for various research problems and operational forecasting, including cloud burst, forest fire, solar power, tropical cyclone and regional climate (Budakoti et al. 2019; Michalakes et al. 2005; Navale et al. 2020; Navale and Singh 2020; Singh et al. 2020). For the simulation of aerosol emission, turbulent mixing, transport and chemical transformation of trace gases and aerosols, a dedicated chemistry module is embedded in the WRF-Chem model (Grell et al. 2005), which has been utilised in this study. NCEP final analysis data with 1° × 1° spatial resolution and 6-h temporal resolution have been used for the model initial and boundary conditions for the simulations. The domain of dust episode simulations in the model is between 0° to 40° N and 50° to 100° E with a horizontal resolution of 25 km. The model configuration considers 41 vertical levels with the height of the lowest layer being 50 m, and the dust-radiative feedback has been enabled in the model. For modelling simulations of dust episodes, WRF-Chem was configured with RRTM for GCM scheme to treat short-wave and longwave radiations within the model (Iacono et al. 2000) and the microphysics option WSM6, Yonsei University (YSU) planetary boundary layer scheme (Hong and Pan 1996). Soil texture data implemented in the model considers 12 texture classes based on FAO (Zobler 1999). The Goddard Global Ozone Chemistry Aerosol Radiation and Transport (GOCART) dust scheme (Ginoux et al. 2001) has been implemented for resolving dust emission and related processes within WRF-Chem simulations. Volume approximation has been used to estimate the optical properties of aerosols. The dust emission is calculated as a function of surface dust inducing variables in the GOCART dust scheme such as surface winds, surface wetness and surface erodibility (Chin et al. 2002). The number of bins considered in the model was 5 with the bin size being 0.5, 1.4, 2.4, 4.5 and 8.0 μm effective radius, respectively.

Reanalysis Dataset

MERRA-2 The Modern-Era Retrospective analysis for Research and Applications version 2 is a global reanalysis which integrates various satellite-based observations with ground and model observations of aerosols. The parameter extracted from the MERRA-2 is Dust load (g/m2), PM10 and PM2.5. The datasets have a spatial resolution of 0.625° X 0.5° and a temporal resolution of 6 h.

Satellite Datasets

MODIS The Aerosol optical depth extracted from the daily level-3 MODIS global atmospheric product at a spatial resolution of 1 degree is used for this particular study. The AOD does not represent the actual quantity of dust in the atmosphere but gives us an idea about the total aerosol in the atmosphere.

OMI The Aerosol Index detects the presence of UV-absorbing aerosols such as dust and soot. UV Aerosol index (AI) is based on a spectral contrast method in a UV region where the ozone absorption is minimal. The measurements of Ozone Monitoring Instrument have a spectral range of 264–504 nm (nanometres) with a spectral resolution between 0.42 nm and 0.63 nm and cover a nominal ground footprint of 13 × 24 sq.km at nadir.

Ground-Based PM10 and PM2.5: Central Pollution Control Board (CPCB) provides data of various parameters over the Indian region. It is a ground-based data collection system. PM10 and PM2.5 data over selected regions in India are considered for validation of model-generated data.

Methods

Qualitative Analysis

Qualitative analysis is done to understand the spatial and temporal distribution of the dust over the study area. An understanding of the general behaviour of the model and that of the dust load is inferred. Qualitative analysis is performed in three steps. The first step is simply a visual interpretation technique in which the model outputs of the same day but for different initial conditions are compared with each other as well as with another dataset to understand the difference in the behaviour of dust due to change in the initial conditions of the model and to assess the accuracy of the model in simulating dust episodes. It can be used to locate the source regions over which dust is emitted. Once the source regions are identified, the variation of dust values at that point over time may be analysed (time-series analysis) to better understand the nature of the dust at the source region.

Additionally, time-series graphs are plotted using Aerosol Optical Depth and Aerosol Index values over the dust episode over the source region. A scatter plot of observational dust values (reanalysis data) with model simulated dust has been generated and the correlation factors are also noted. Time-series graphs for PM10 and PM2.5 values over parts of India during the time in which dust episodes occurred serves to explain whether there is any influence of the dust storms in Arabian Peninsula on the air quality over India.

Quantitative Analysis

In this study, to develop a quantitative understanding of the model data, a probability density function and cumulative density function were plotted using the model data and the MERRA-2 data. The probability distribution function helps us understand how the model values are assigned compared to the same location in the observation datasets, i.e. count of each value and how it differs in both the datasets. The cumulative distribution helps to assess the pattern of both the datasets and to assess how different it is from each other. Various significance tests can be performed to analyse the difference between the datasets. Categorical Statistics of the datasets were carried out not to understand the intensity of values but to understand how well the model has performed in capturing the data points. The statistical metrics used for this has been given in a 2 X 2 contingency table as shown in Table 1. Various scores can be calculated using the formulas stated below (Bharti and Singh 2015; Navale et al. 2020; Navale and Singh 2020a).

Probability of Detection (hit rate): It tells how well the model estimated multiple dust events (hits). The value lies between 0 and 1 with 1 being the desired result.

$$POD = \frac{a}{a+c}$$

Critical Success Index (CSI) It is the fraction of correctly estimated dust events by model, i.e. the accuracy with which the model gives hits (correct dust events),

Table 1 Contingency table used to evaluate the performance of WRF-Chem model in detecting dust events

	MERRA-2 dust	MERRA-2 no dust
WRF dust	a (hit)	b (false alarm)
WRF no dust	c (miss)	d (no correction)
Total	a + b + c + d	

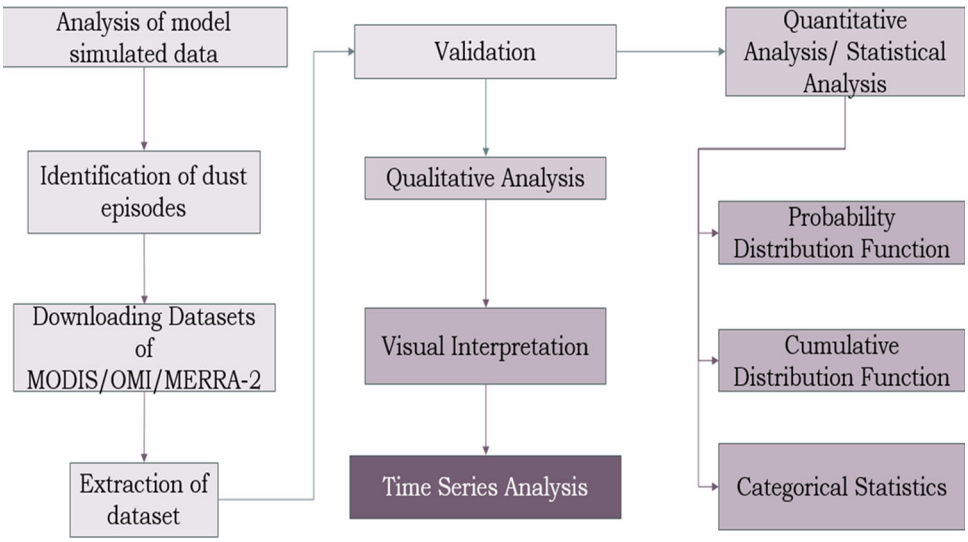

Fig. 2 Flowchart of methodology followed for this study

Table 2 Identified dust episodes during post-monsoon of 2018

Dust Events	Duration (h)	Location	Number of Time Steps
11th October 2018	12–24	Arabian Peninsula	28
19th October 2018	24–36	Arabian Peninsula	28
30th October 2018	18–36	Arabian Peninsula, Afghan Coast	28
4th November 2018	48	Arabian Peninsula	28
13th November 2018	12–18	Arabian Peninsula	28

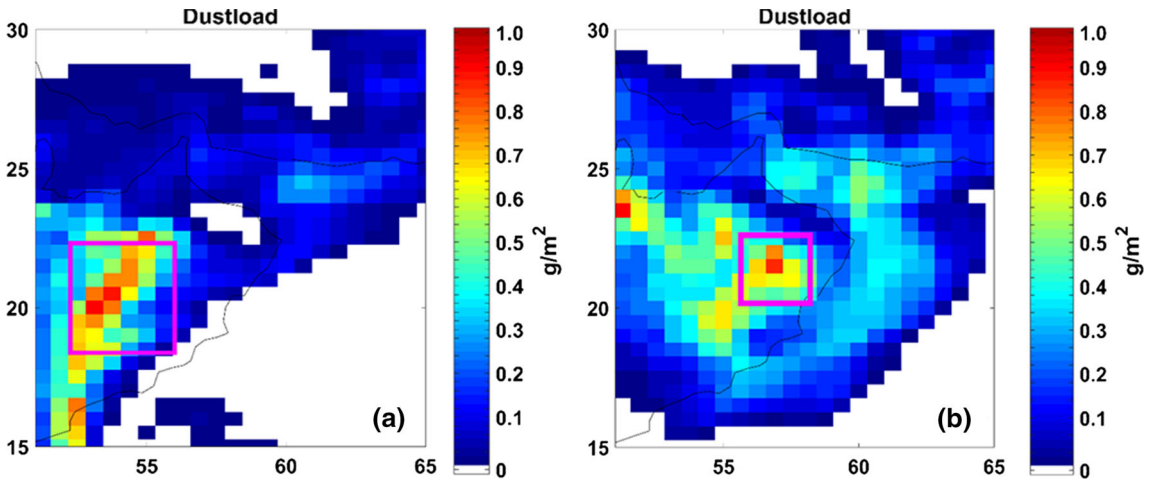

Fig. 3 WRF-CHEM simulated dust load over dust source region of dust event on **a** 11th October 2018 and **b** 4th November 2018

although correct no-dust events are not considered. The value ranges from 0 to 1 with 1 as the perfect score.

$$CSI = \frac{a}{a+b+c}$$

Accuracy It measures how much model and satellites agree on detection of dust events. The ideal score is 1.

$$Accuracy = \frac{a+d}{Total}$$

False Alarm Ratio (FAR) The false alarm is the ratio of falsely detected dust pixels divided by total dust pixels as estimated by the model. For best results, it should be near or equal to zero.

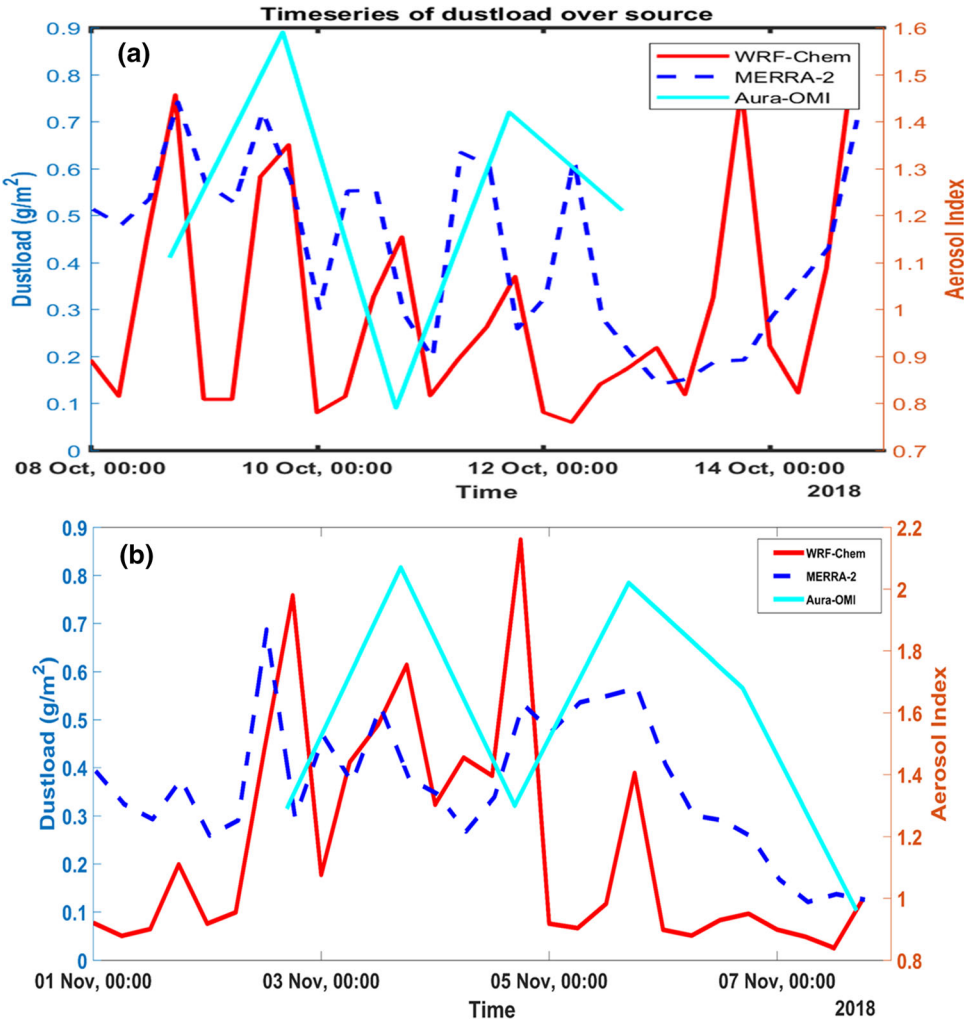

Fig. 4 Time-series plot showing dust load and aerosol index for dust event on **a** 11th October 2018 and **b** 4th November 2018

$$FAR = \frac{b}{a+b}$$

Frequency Bias Index (FBI) The ratio of model-estimated events to the observed events measures whether the model is overestimating or underestimating the frequency of dust events. The desired score is 1 with value lesser or greater than 1 indicating underestimation or overestimation of the frequency of dust events, respectively.

$$FBI = \frac{a+b}{a+c}$$

The methodology followed for this study has been shown in Fig. 2.

Results and Discussions

Identification of Dust Events

The standard statistical measurements exhibit some striking features of the WRF-Chem model over the source regions. The effect of dust emitted over the Arabian Peninsula is maximum during the pre-monsoon and post-monsoon period. This effect is mainly due to the strong Shamal winds which are the north-westerlies which are active during this period. These winds carry dust particles emitted over the Arabian Peninsula to the Indian subcontinent. In this study, dust episodes which took place during the post-monsoon season are considered, particularly the months of October and November of the year 2018.

The various dust storm events, which are also called the dust episodes, were identified from various literatures (newspaper and research articles) and were confirmed using MODIS-Terra optical datasets. From these 5–6 events were observed to be dust storms. These events are

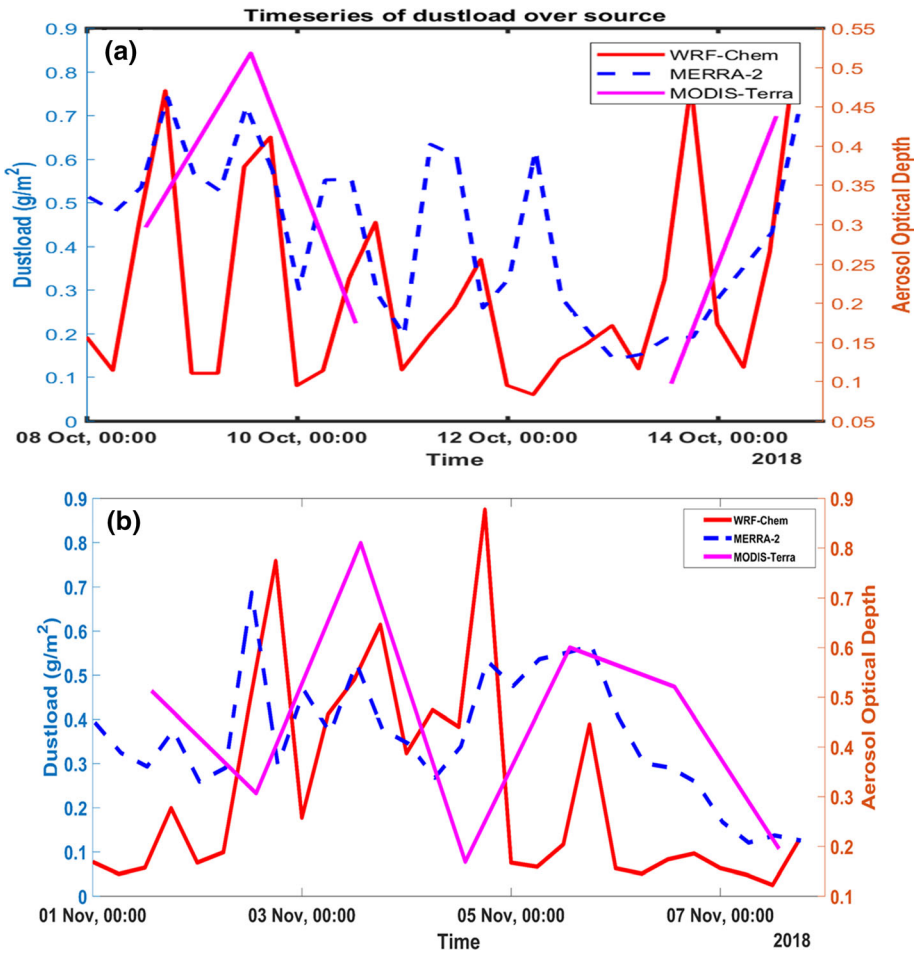

Fig. 5 Time-series plot showing dust load and aerosol optical depth for dust episode on **a** 11th October 2018 and **b** 4th November 2018

listed in Table 2. Most of the dust storms took place over the Arabian Peninsula; however, a few dust events of a smaller scale were observed over the Afghanistan-Pakistan border. The smaller scale and duration of these events are, nevertheless, quite significant in terms of air quality over the Indian region.

Qualitative Analysis

An initial analysis of the general behaviour of the model showed its ability to estimate dust value over the entire spatial extent of the study area. Following this, a more detailed analysis was taken up by considering each dust episode separately and for the source region of that particular event. For this, a particular area of the source region was selected and isolated for each region which corresponds to the location from where the dust was emitted. Time-series plots and scatterplots were plotted using the pixel values of both WRF model data and MERRA-2 from the source region. Time-series plots of PM10 and PM2.5, using both model data and ground observations, help understand the effect of these dust events over the Indian subcontinent.

11th October 2018

A dust event was identified to have formed during the days of 8th to 14th October 2018 over the Arabian Peninsula. The number of times-steps considered was 28 for WRF-Chem and MERRA-2, whereas for OMI and MODIS it was 7. Figure 3a shows the location which has been taken for the analysis of this particular day. The extent of this is between 19° N to 22.5° N and 52.5° E to 56.88° E.

Figure 4a shows the temporal evolution of dust concentration in the air. Both WRF-Chem and MERRA-2 values are represented here along with the aerosol index. The WRF-Chem model does a decent job in capturing the pattern of the change in dust concentration as signified by the match between most of the peaks between the model and the observational data. The slight mismatch in the location of the peaks between the different datasets may be due to the difference in the time interval between successive acquisition or simulation. The aerosol index data of the Aura-OMI also show a nearly similar pattern even though the number of time-steps has reduced. Figure 5a also shows the evolution of dust concentration along with aerosol optical depth. AOD data from MODIS-Terra also

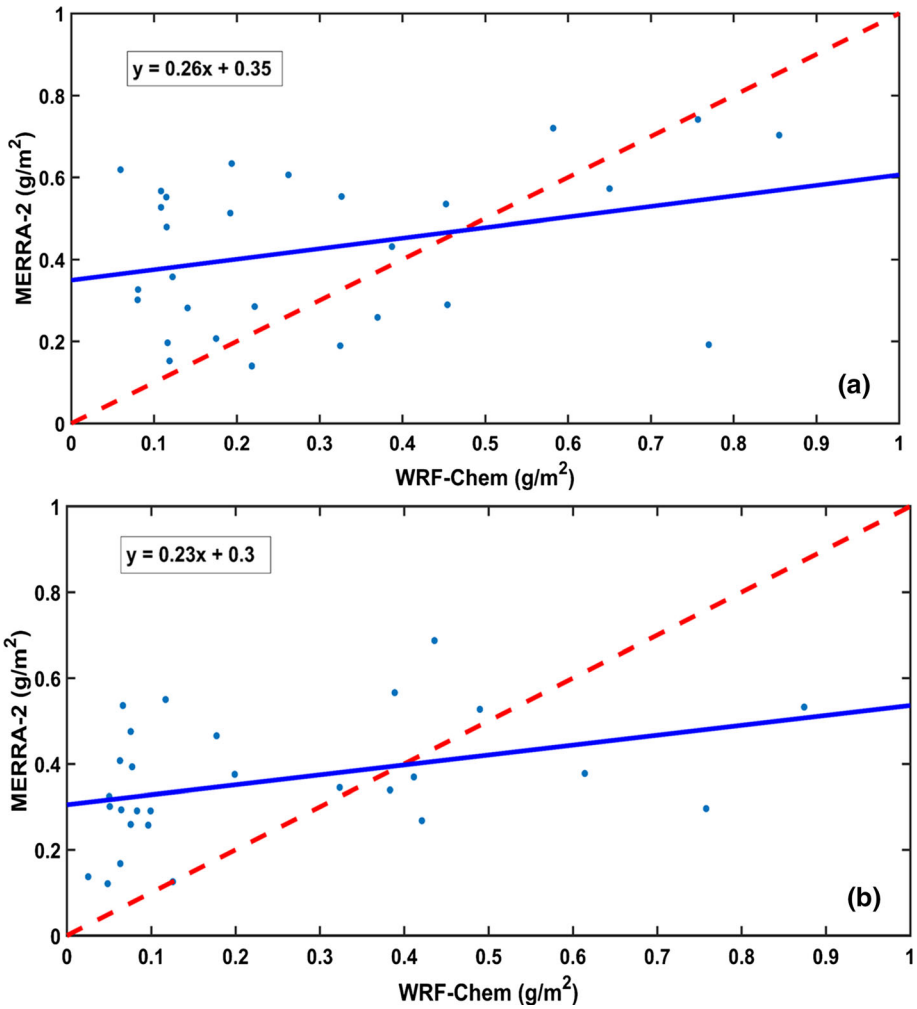

Fig. 6 Scatterplot of MERRA-2 vs WRF-Chem for dust episode on **a** 11th October 2018 and **b** 4th November 2018

show an excellent match with the WRF-Chem pattern. The WRF-Chem simulations show consistent lower values throughout the entire event. This agrees with the observations from the spatial maps that the WRF-Chem model is consistently underestimating the dust values compared to values of the observation dataset.

Figure 6a shows the relationship between the observation data set and the model dataset. The dotted line represents the reference line along which there is a one-to-one relationship between the two datasets. The relation depicted by this line is the one that is desired. However, the blue line shows the actual relation between the model dataset and the observation dataset. Since it differs significantly from the reference line, we can infer that there is a considerable difference between the intensity of values estimated by the model data and that of observational data. The data points lying above the reference line show that the WRF-Chem model mostly highly underestimates them. This supports the observations from the spatial maps and time-series plots of the model datasets. On further observation, we also notice that the underestimation is more prominent for smaller values, whereas the higher values are not affected much. The coefficients to correct this underestimation have also been estimated. The sensitivity of the model in estimating the PM10 and PM2.5 has also been explored as shown in Fig. 7a and Fig. 8a, respectively. The time-series plots of concentration of particulate matter have been plotted and compared with ground measurements over New Delhi to understand the effects of dust storm events over the Arabian Peninsula on the air quality over the Indian region. A considerable increase in the concentration of both PM10 and PM2.5 a couple of days after a dust episode is observed. This shows that there is a positive relationship between the dust storms over Arabia and the air quality over India.

The WRF model can capture the intensity of the PM10 quite well. There is a peak for both WRF and the ground data on 13th October which is two days after the dust episode on 11th October over the Arabian Peninsula. However, for PM2.5, it seems that there is an underestimation by the WRF model. However, this is maybe because the WRF-Chem model is being to simulate only

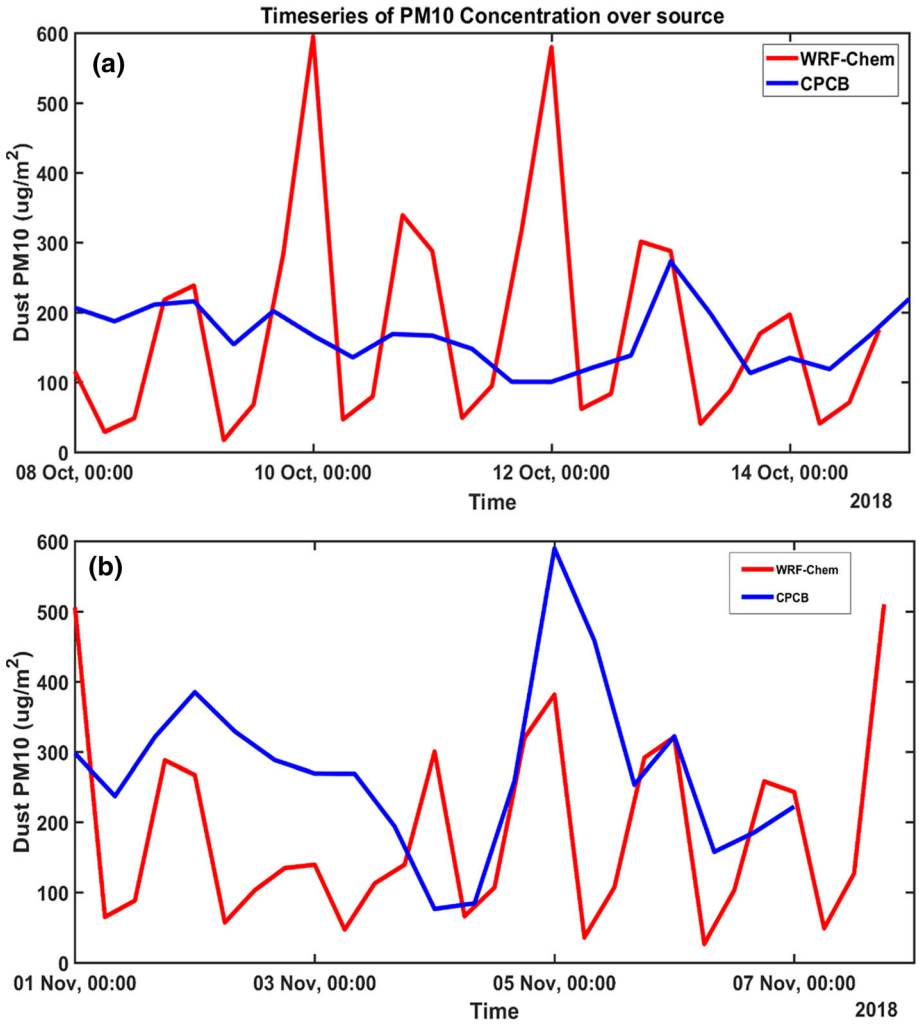

Fig. 7 Time-Series plot of PM10 over New Delhi on **a** 11th October 2018 and **b** 4th November 2018

dust and its peak over 13th October represents PM2.5 contribution from dust alone, whereas the peak for the measured data for the same date shows PM2.5 contribution from multiple sources. In the case of PM10, there is only a small difference between the values estimated by the model and the observation data, particularly during 13th October 2018 where the peaks match very well. The reason for this is that dust particles are one of the main contributors to PM10, and it does not contribute much to PM2.5.

4th November 2018

During the days of 8th to 14th October 2018 over the Arabian Peninsula, a dust episode had taken place. The number of times-steps that considered was 28 for WRF-Chem and MERRA-2, whereas for OMI and MODIS it was 7. Figure 3b shows the location which has been taken for the analysis of this particular day. The extent of this is between 20.5° N to 22.5° N and 56.25° E to 58.13° E.

Figures 4b and 5b show the temporal evolution of the concentration of dust in the atmosphere based on the WRF-Chem model and MERRA-2 datasets along with the aerosol index values from Aura OMI and AOD values from MODIS-Terra, for the dust event on 4th November 2018. Here also the three datasets show a significant positive correlation. Furthermore, the WRF-Chem model depicts on an average a lower value of dust, a behaviour which is observed in multiple dust event simulations. A scatterplot for the same datasets of the same period is also shown in Fig. 6b. Here also we can see that the behaviour of the dataset is consistent with the previously discussed event as well as with the other events. In Fig. 6b, all the datapoints with lower values are lying above the reference line which means that all the lower values are underestimated and some data points having higher values lie below the reference line which shows that the WRF model overestimates higher values. The values of PM10 and PM2.5 over New Delhi were also plotted to understand how they change over time for this particular dust event. There is a

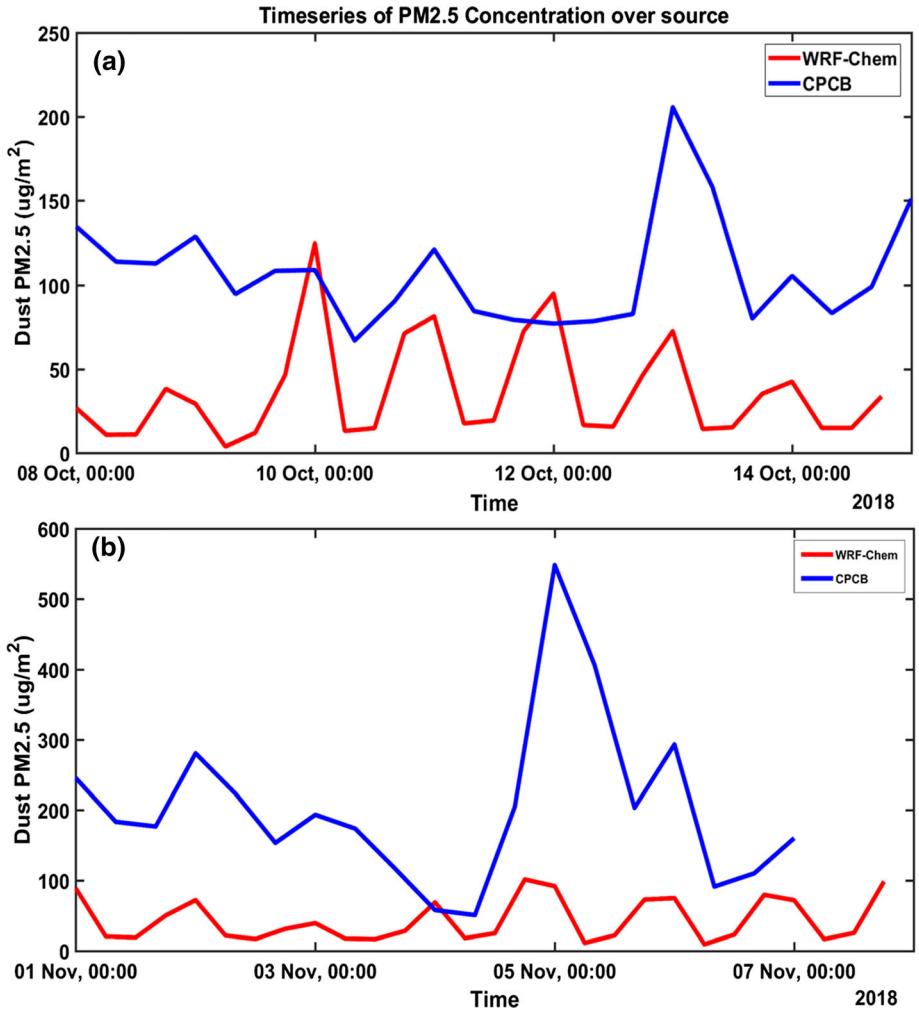

Fig. 8 Time-Series of PM2.5 over New Delhi on **a** 11th October 2018 and **b** 4th November 2018

sharp hike in PM10 values on 5th November 2018 followed by a dust episode on the 3rd and 4th of November 2018 which can be observed in the time-series plot shown in Fig. 7b. The ground values show higher values on 5th November compared to the model-generated values. This could be because there might have been other sources than dust for PM10 during that period in that region. The scatter plot of PM2.5 shown in Fig. 8b shows a pattern that is similar to that of the previously discussed dust event with the model values depicting highly underestimated values compared to the measured values. The consistent lower values are because dust does not contribute much to PM2.5. However, there is an excellent correlation between the pattern of the two time-series plots.

Quantitative Analysis

For the same dust events, quantitative analysis has also been performed. Probability distribution function (PDF) and cumulative distribution function (CDF) have also been plotted for these events. The PDF helps us to understand how the data is distributed in terms of value. It can be compared with observation datasets to understand how well the WRF model captures the values. The CDF is also used here to find how much the model data varies from the observed data. Some significance tests can be performed on these PDFs and CDFs to serve as a test to find the goodness of fit. Figure 9a shows the plot probability distribution function of the WRF model-generated data and MERRA-2 data for the dust episode, which took place on 11th October 2018. From the PDF of MERRA-2, we know the actual distribution of the of data points. There is a considerable variation of values estimated by the WRF model from the observational data, particularly in the case of lower values where there are more data points with lower magnitude. This again supports the previous observations that the model is underestimating the lower values. As we move towards the higher values, it is seen that the frequency of the model and observation datasets match. Similar observations are noted in Fig. 9b, which is the PDF plotted for the dust event on 4th November 2018. Here also the WRF model underestimates the dust values at lower values and

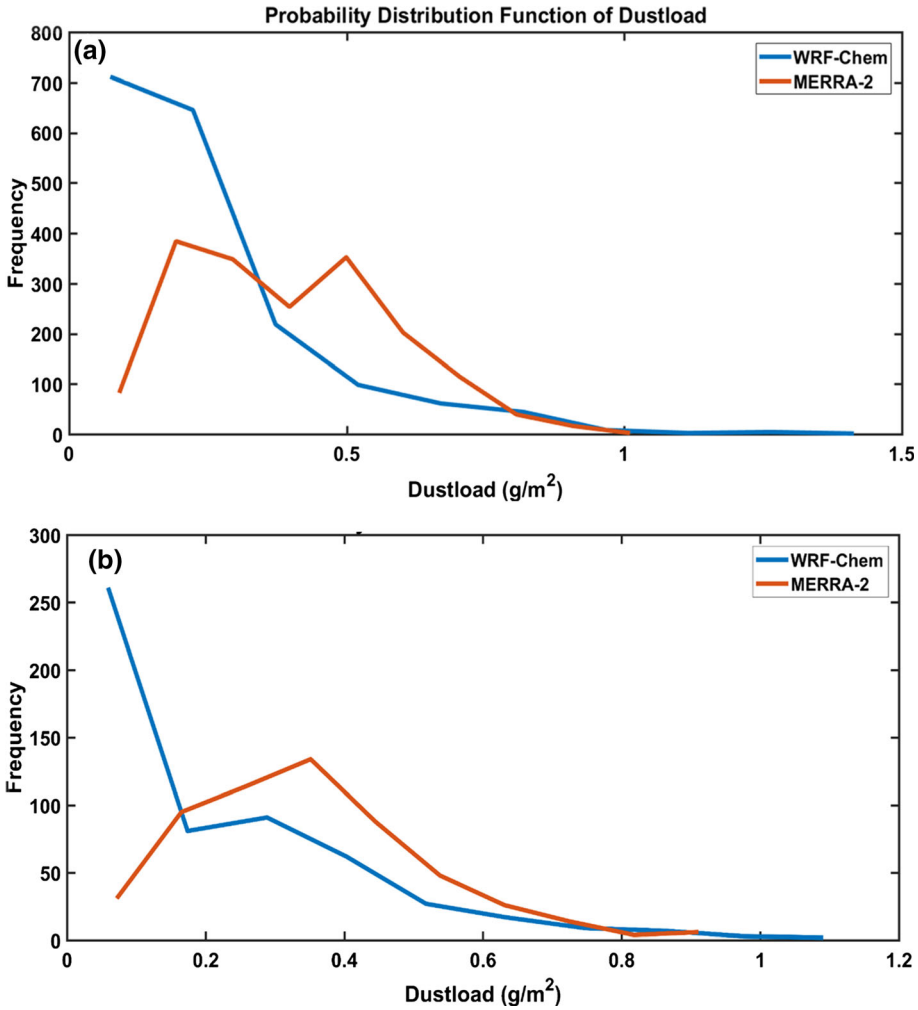

Fig. 9 PDF plot for **a** 11th October 2018 and **b** 4th November 2018

matches at the higher values. Figure 10 depicts the cumulative distribution function for model and observational data for the 11th October and 4th November of 2018. The shift in the curves of model data from the observational dataset as well as the difference in the pattern which is seen in both the plots shows that the model data varies significantly from the observations. We have utilised here Kolomogorov Smirnov test (KS-test) for the comparison of CDFs of two data sets following previous studies (Singh 2013; Singh et al. 2017a; Kundu and Singh 2020). Additionally, the results of the significance test (K-S test) performed using these plots also show a considerable mismatch between the two datasets. A categorical analysis was also done on these to understand whether or not the model was able to capture the dust events accurately.

Likewise, analysis of other events has also been carried out and results based on categorical validation are mentioned. Table 3 shows the score for all six events that were analysed for each parameter which helps in determining the effectiveness of the WRF-Chem model. Here Probability of Detection (Hit rate) for 11th October is 94% which shows that the model estimates the dust values quite well for this event. However, for the 19th of the same month is 55% which means the hit rate has significantly reduced for that event. The highest accuracies were observed for the dust episodes on 11th October and 4th November. The simulation with most desired FAR values was that simulated on 30th October over the Arabian Peninsula.

Conclusion

The study aims to assess the output of WRF-Chem simulated dust using different satellite, reanalysis and ground-based observation data sets. The output of this model is used for various operations, including air quality monitoring, weather prediction, and to understand the effects of the dust on the air quality of the Indian region. The use of this model output in various critical operations has made it necessary that the model is accurate and precise. In this study, the model data are analysed and validated using other satellite and ground-based observational products.

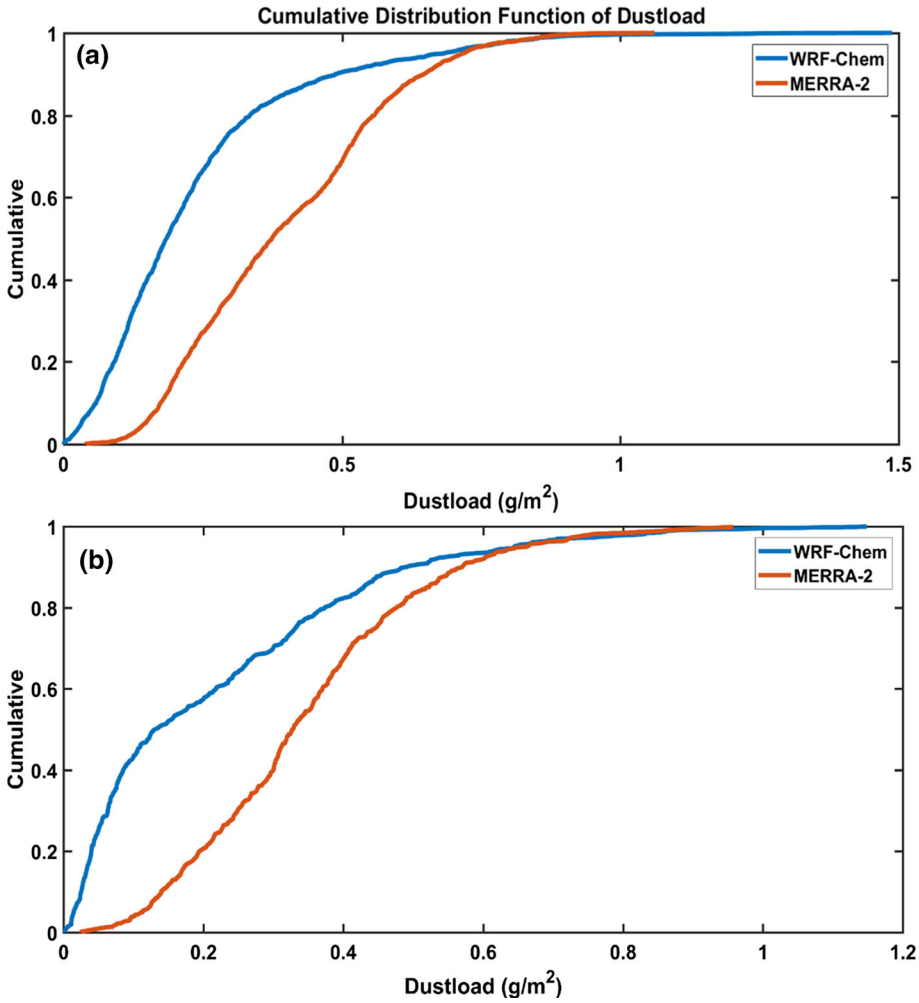

Fig. 10 CDF plot for **a** 11th October 2018 and **b** 4th November 2018

Table 3 Results of categorical analysis of the dust episodes

	11th October 2018 Arabian Peninsula	19th October 2018 Arabian Peninsula	30th October 2018		4th November 2018 Arabian Peninsula	13th November 2018 Arabian Peninsula	Average
			Arabian Peninsula	Afghan Coast			
POD	0.94	0.56	0.71	0.81	0.80	0.79	0.77
CSI	0.82	0.50	0.69	0.74	0.75	0.53	0.67
FAR	0.14	0.17	0.03	0.11	0.08	0.38	0.15
Accuracy	0.83	0.68	0.72	0.79	0.82	0.73	0.76
FBI	1.09	0.67	0.73	0.91	0.87	1.29	0.93

The primary dataset that was used was dust load data from MERRA-2 and was chosen as the primary reference because both the model and the measurement data have the same parameters (i.e. dust load). The other parameters that were used are aerosol optical depth from MODIS-Terra and aerosol index from Aura-OMI, which was used as supplementary measurements. The model-generated PM10, and PM2.5 were also compared with the ground measurements of particulate matter by CPCB. This study was performed for October and November (i.e. post-monsoon season) as it is one of the periods during which dust activity is at its maximum and has observed to influence the air quality over India. Based on the satellite observations, it is noted that the WRF-Chem model being run to estimate the

dust load in the atmosphere is able to capture the values reasonably well for the post-monsoon season.

The magnitude of PM10 and PM2.5 generated by the model also agrees with the previous studies which link dust storms over the middle east and Indian region. Statistical analysis has been performed on the datasets to validate the performance of the model and to assess the intensity of the estimated values. Plots for probability distribution function, cumulative distribution functions, temporal evolution, and scatter plot consistently show that the WRF-Chem model underestimates the amount of dust over all the dust events. It is also noted that the WRF-Chem model can successfully capture the entire dust cycle (which includes the emission, transportation and dissipation) reasonably well. The categorical analysis was also performed for each dust episode, and the average values for Probability of Detection are 77%, Critical Success Index is 67%, false alarm ratio is 15%, and Frequency Bias Index is 92% with an overall accuracy of 76% which shows an above-average performance of the model. In the current work, the performance of the model for six dust episodes has been analysed, and there is a need to calibrate the model output using satellite data before it is used for any purpose. More comprehensive work with more dust episodes and a variety of statistical tests may be carried out in the future for detailed evaluation.

Acknowledgement Present work is a part of TDP and AR, CS and SKS are thankful to Group Head MASD, Dean (Academics) for the support and encouragement. Various data sets have been utilised in the present study such as MERRA-2, MODIS-Terra, Aura-OMI, CPCB (Ground-based Aerosol Product) and we thank respective data providers and science team for preparing the quality-controlled data sets and making it available free of cost for research purpose.

Funding Not Applicable.

Compliance with Ethical Standards

Conflicts of interest The authors declared that they have no conflict of interest.

Availability of Data and Material Data available with authors.

References

Ackerman, A. S., Toon, O. B., Stevens, D. E., Heymsfield, A. J., Ramanathan, V., & Welton, E. J. (2000). Reduction of tropical cloudiness by soot. *Science, 288*(5468), 1042–1047. https://doi.org/10.1126/science.288.5468.1042.

Alonso-Pérez, S., Cuevas, E., Querol, X., Guerra, J. C., & Pérez, C. (2012). African dust source regions for observed dust outbreaks over the Subtropical Eastern North Atlantic region, above 25°N. *Journal of Arid Environments, 78,* 100–109. https://doi.org/10.1016/j.jaridenv.2011.11.013.

Andreae, M. O., Charlson, R. J., Bruynseels, F., Storms, H., van Grieken, R., & Maenhaut, W. (1986). Internal mixture of sea salt, silicates, and excess sulfate in marine aerosols. *Science, 232*(4758), 1620–1623.

Bharti, V., & Singh, C. (2015). Evaluation of error in TRMM 3B42V7 precipitation estimates over the Himalayan region. *Journal of Geophysical Research: Atmospheres, 120*(24), 12458–12473. https://doi.org/10.1002/2015JD023779.

Bolin, B., Aspling, G., & Persson, C. (1974). Residence time of atmospheric pollutants as dependent on source characteristics, atmospheric diffusion processes and sink mechanisms. *Tellus, 26*(1–2), 185–195. https://doi.org/10.3402/tellusa.v26i1-2.9772.

Budakoti, S., Singh, C., & Pal, P. K. (2019). Assessment of various cumulus parameterization schemes for the simulation of very heavy rainfall event based on optimal ensemble approach. *Atmospheric Research, 218,* 195–206. https://doi.org/10.1016/j.atmosres.2018.12.005.

Cavazos-Guerra, C., & Todd, M. C. (2012). Model Simulations of complex dust emissions over the Sahara during the West African monsoon onset. *Advances in Meteorology*. https://doi.org/10.1155/2012/351731.

Chin, M., Ginoux, P., Kinne, S., Torres, O., Holben, B. N., Duncan, B. N., et al. (2002). Tropospheric aerosol optical thickness from the GOCART model and comparisons with satellite and sun photometer measurements. *Journal of Atmospheric Sciences, 59*(3), 461–483. https://doi.org/10.1175/1520-0469(2002)059%3c0461:TAOTFT%3e2.0.CO;2.

Choobari, O. A., Zawar-Reza, P., & Sturman, A. (2014). The global distribution of mineral dust and its impacts on the climate system: A review. *Atmospheric Research, 138,* 152–165. https://doi.org/10.1016/j.atmosres.2013.11.007.

Dey, S., Tripathi, S. N., Singh, R. P., & Holben, B. N. (2004). Influence of dust storms on the aerosol optical properties over the Indo-Gangetic basin. *Journal of Geophysical Research Atmospheres*. https://doi.org/10.1029/2004JD004924.

Dubovik, O., Holben, B., Eck, T. F., Smirnov, A., Kaufman, Y. J., King, M. D., et al. (2002). Variability of absorption and optical properties of key aerosol types observed in worldwide locations. *Journal of the Atmospheric Sciences, 59*(3), 590–608. https://doi.org/10.1175/1520-0469(2002)059%3c0590:VOAAOP%3e2.0.CO;2.

Dumka, U. C., Kaskaoutis, D. G., Francis, D., Chaboureau, J.-P., Rashki, A., Tiwari, S., et al. (2019). The role of the intertropical discontinuity region and the heat low in dust emission and transport over the Thar desert, India: A premonsoon case study. *Journal of Geophysical Research: Atmospheres, 124*(23), 13197–13219. https://doi.org/10.1029/2019JD030836.

Durant, A. J., Harrison, S. P., Watson, I. M., & Balkanski, Y. (2009). Sensitivity of direct radiative forcing by mineral dust to particle characteristics. *Progress in Physical Geography*. https://doi.org/10.1177/0309133309105034.

Engelstaedter, S., Tegen, I., & Washington, R. (2006). North African dust emissions and transport. *Earth-Science Reviews, 79*(1), 73–100. https://doi.org/10.1016/j.earscirev.2006.06.004.

Ginoux, P., Chin, M., Tegen, I., Prospero, J. M., Holben, B., Dubovik, O., & Lin, S.-J. (2001). Sources and distributions of dust aerosols simulated with the GOCART model. *Journal of Geophysical Research Atmospheres, 106*(D17), 20255–20273. https://doi.org/10.1029/2000JD000053.

Ginoux, P., Prospero, J. M., Torres, O., & Chin, M. (2004). Long-term simulation of global dust distribution with the GOCART model: Correlation with North Atlantic Oscillation. *Environmental Modelling & Software, 19*(2), 113–128. https://doi.org/10.1016/S1364-8152(03)00114-2.

Ginoux, P., Prospero, J. M., Gill, T. E., Hsu, N. C., & Zhao, M. (2012). Global-scale attribution of anthropogenic and natural

dust sources and their emission rates based on MODIS Deep Blue aerosol products. *Reviews of Geophysics*. https://doi.org/10.1029/2012RG000388.

Gong, S. L., Lavoué, D., Zhao, T. L., Huang, P., & Kaminski, J. W. (2012). GEM-AQ/EC, an on-line global multi-scale chemical weather modelling system: Model development and evaluation of global aerosol climatology. *Atmospheric Chemistry and Physics, 12*(17), 8237–8256. https://doi.org/10.5194/acp-12-8237-2012.

Goudie, A., & Middleton, N. J. (2006). *Desert dust in the global system*. Berlin Heidelberg: Springer-Verlag. https://doi.org/10.1007/3-540-32355-4.

Grell, G. A., Peckham, S. E., Schmitz, R., McKeen, S. A., Frost, G., Skamarock, W. C., & Eder, B. (2005). Fully coupled "online" chemistry within the WRF model. *Atmospheric Environment, 39*(37), 6957–6975. https://doi.org/10.1016/j.atmosenv.2005.04.027.

Griffin, D. W., Kellogg, C. A., Garrison, V. H., & Shinn, E. A. (2002). The global transport of dust: An intercontinental river of dust, microorganisms and toxic chemicals flows through the earth's atmosphere. *American Scientist, 90*(3), 228–235.

Gunn, R., & Phillips, B. B. (1957). AN Experimental investigation of the effect of air pollution on the initiation of rain. *Journal of Meteorology, 14*(3), 272–280. https://doi.org/10.1175/1520-0469(1957)014%3c0272:AEIOTE%3e2.0.CO;2.

Hansell, R. A., Tsay, S. C., Ji, Q., Hsu, N. C., Jeong, M. J., Wang, S. H., et al. (2010). An assessment of the surface longwave direct radiative effect of airborne Saharan dust during the NAMMA field campaign. *Journal of the Atmospheric Sciences, 67*(4), 1048–1065. https://doi.org/10.1175/2009JAS3257.1.

Hansen, J., Sato, M., & Ruedy, R. (1997). Radiative forcing and climate response. *Journal of Geophysical Research: Atmospheres, 102*(D6), 6831–6864. https://doi.org/10.1029/96JD03436.

Hong, S.-Y., & Pan, H.-L. (1996). Nonlocal boundary layer vertical diffusion in a medium-range forecast model. *Monthly Weather Review, 124*(10), 2322–2339. https://doi.org/10.1175/1520-0493(1996)124%3c2322:NBLVDI%3e2.0.CO;2.

Iacono, M. J., Mlawer, E. J., Clough, S. A., & Morcrette, J.-J. (2000). Impact of an improved longwave radiation model, RRTM, on the energy budget and thermodynamic properties of the NCAR community climate model, CCM3. *Journal of Geophysical Research: Atmospheres, 105*(D11), 14873–14890. https://doi.org/10.1029/2000JD900091.

Iii, C. A. P., Burnett, R. T., Thun, M. J., Calle, E. E., Krewski, D., Ito, K., & Thurston, G. D. (2002). Lung cancer, cardiopulmonary mortality, and long-term exposure to fine particulate air pollution. *JAMA, 287*(9), 1132–1141. https://doi.org/10.1001/jama.287.9.1132.

Jickells, T. D., An, Z. S., Andersen, K. K., Baker, A. R., Bergametti, G., Brooks, N., et al. (2005). global iron connections between desert dust, ocean biogeochemistry, and climate. *Science, 308*(5718), 67–71. https://doi.org/10.1126/science.1105959.

Jin, Q., Wei, J., Yang, Z.-L., Pu, B., & Huang, J. (2015). Consistent response of Indian summer monsoon to Middle East dust in observations and simulations. *Atmospheric Chemistry and Physics, 15*(17), 9897–9915. https://doi.org/10.5194/acp-15-9897-2015.

Jin, Q., Wei, J., & Yang, Z.-L. (2014). Positive response of Indian summer rainfall to Middle East dust. *Geophysical Research Letters, 41*(11), 4068–4074. https://doi.org/10.1002/2014GL059980.

Jing, Su., Huang, J., Qiang, Fu., Minnis, P., Ge, J., & Bi, J. (2008). Estimation of Asian dust aerosol effect on cloud radiation forcing using Fu-Liou radiative model and CERES measurements. *Atmospheric Chemistry and Physics, 8*(10), 2763–2771. https://doi.org/10.5194/acp-8-2763-2008.

Kaufman, Y. J., Koren, I., Remer, L. A., Tanré, D., Ginoux, P., & Fan, S. (2005). Dust transport and deposition observed from the Terra-Moderate Resolution Imaging Spectroradiometer (MODIS) spacecraft over the Atlantic Ocean. *Journal of Geophysical Research: Atmospheres*. https://doi.org/10.1029/2003JD004436.

Kedia, S., Kumar, R., Islam, S., Sathe, Y., & Kaginalkar, A. (2018). Radiative impact of a heavy dust storm over India and surrounding oceanic regions. *Atmospheric Environment, 185,* 109–120. https://doi.org/10.1016/j.atmosenv.2018.05.005.

Koren, I., Kaufman, Y. J., Remer, L. A., & Martins, J. V. (2004). Measurement of the effect of Amazon smoke on inhibition of cloud formation. *Science, 303*(5662), 1342–1345. https://doi.org/10.1126/science.1089424.

Kumar, R., Barth, M. C., Pfister, G. G., Naja, M., & Brasseur, G. P. (2014). WRF-Chem simulations of a typical pre-monsoon dust storm in northern India: Influences on aerosol optical properties and radiation budget. *Atmospheric Chemistry and Physics, 14*(5), 2431–2446. https://doi.org/10.5194/acp-14-2431-2014.

Kundu, S. K., & Singh, C. (2020). Rainfall pattern over the North-West Himalayan region: historical time period vs. future warming scenarios. *Theoretical and Applied Climatology, 141*(1), 257–269. https://doi.org/10.1007/s00704-020-03210-7.

Liou, K.-N., & Ou, S.-C. (1989). The role of cloud microphysical processes in climate: An assessment from a one-dimensional perspective. *Journal of Geophysical Research: Atmospheres, 94*(D6), 8599–8607. https://doi.org/10.1029/JD094iD06p08599.

McCormick, R. A., & Ludwig, J. H. (1967). Climate modification by atmospheric aerosols. *Science, 156*(3780), 1358–1359. https://doi.org/10.1126/science.156.3780.1358.

McGowan, H. A., & Soderholm, J. (2012). Laser ceilometer measurements of Australian dust storm highlight need for reassessment of atmospheric dust plume loads. *Geophysical Research Letters*. https://doi.org/10.1029/2011GL050319.

Michalakes, J., Dudhia, J., Gill, D., Henderson, T., Klemp, J., Skamarock, W., & Wang, W. (2005). The weather research and forecast model: software architecture and performance. *Use of High Performance Computing in Meteorology*. https://doi.org/10.1142/9789812701831_0012.

Middleton, N. J. (1986). A geography of dust storms in South-West Asia. *Journal of Climatology, 6*(2), 183–196. https://doi.org/10.1002/joc.3370060207.

Miller, R. L., & Tegen, I. (1998). Climate response to soil dust aerosols. *Journal of Climate, 11*(12), 3247–3267. https://doi.org/10.1175/1520-0442(1998)011%3c3247:CRTSDA%3e2.0.CO;2.

Miller, R. L., Tegen, I., & Perlwitz, J. (2004). Surface radiative forcing by soil dust aerosols and the hydrologic cycle. *Journal of Geophysical Research: Atmospheres*. https://doi.org/10.1029/2003JD004085.

Nabavi, S. O., Haimberger, L., & Samimi, C. (2017). Sensitivity of WRF-chem predictions to dust source function specification in West Asia. *Aeolian Research, 24,* 115–131. https://doi.org/10.1016/j.aeolia.2016.12.005.

Navale, A., & Singh, C. (2020). Topographic sensitivity of WRF-simulated rainfall patterns over the North West Himalayan region. *Atmospheric Research, 242,* 105003. https://doi.org/10.1016/j.atmosres.2020.105003.

Navale, A., Singh, C., Budakoti, S., & Singh, S. K. (2020). Evaluation of season long rainfall simulated by WRF over the NWH region: KF vs. *MSKF*. *Atmospheric Research, 232,* 104682. https://doi.org/10.1016/j.atmosres.2019.104682.

Orlovsky, L., Orlovsky, N., & Durdyev, A. (2005). Dust storms in Turkmenistan. *Journal of Arid Environments, 60*(1), 83–97. https://doi.org/10.1016/j.jaridenv.2004.02.008.

Pease, P. P., Tchakerian, V. P., & Tindale, N. W. (1998). Aerosols over the Arabian Sea: Geochemistry and source areas for aeolian desert dust. *Journal of Arid Environments, 39*(3), 477–496. https://doi.org/10.1006/jare.1997.0368.

Prospero, J. M. (1999). Long-term measurements of the transport of African mineral dust to the southeastern United States: Implications for regional air quality. *Journal of Geophysical Research: Atmospheres, 104*(D13), 15917–15927. https://doi.org/10.1029/1999JD900072.

Prospero, J. M., Ginoux, P., Torres, O., Nicholson, S. E., & Gill, T. E. (2002). Environmental Characterization of Global Sources of Atmospheric Soil Dust Identified with the Nimbus 7 Total Ozone Mapping Spectrometer (toms) Absorbing Aerosol Product. *Reviews of Geophysics*. https://doi.org/10.1029/2000RG000095.

Rajot, J. L., Formenti, P., Alfaro, S., Desboeufs, K., Chevaillier, S., Chatenet, B., et al. (2008). AMMA dust experiment: An overview of measurements performed during the dry season special observation period (SOP0) at the Banizoumbou (Niger) supersite. *Journal of Geophysical Research Atmospheres*. https://doi.org/10.1029/2008JD009906.

Santos, D., Costa, M. J., Silva, A. M., & Salgado, R. (2013). Modeling Saharan desert dust radiative effects on clouds. *Atmospheric Research, 127,* 178–194. https://doi.org/10.1016/j.atmosres.2012.09.024.

Science, G. (2020). Anatomy of a severe dust storm in the Middle East: Impacts on aerosol optical properties and radiation budget. *Aerosol and Air Quality Research, 20*(1), 155–165. https://doi.org/10.4209/aaqr.2019.04.0165.

Shao, Y. (Ed.). (2009). *Physics and modelling of wind erosion*. Netherlands: Springer.

Singh, C. (2013). Changing pattern of the Indian summer monsoon rainfall: an objective analysis. *Climate Dynamics, 41*(1), 195–203. https://doi.org/10.1007/s00382-013-1710-3.

Singh, C., Ganguly, D., & Dash, S. K. (2017a). Dust load and rainfall characteristics and their relationship over the South Asian monsoon region under various warming scenarios. *Journal of Geophysical Research: Atmospheres, 122*(15), 7896–7921. https://doi.org/10.1002/2017JD027451.

Singh, C., Ganguly, D., & Dash, S. K. (2018). On the dust load and rainfall relationship in South Asia: An analysis from CMIP5. *Climate Dynamics, 50*(1–2), 403–422. https://doi.org/10.1007/s00382-017-3617-x.

Singh, C., Ganguly, D., & Sharma, P. (2019a). Impact of West Asia, Tibetan Plateau and local dust emissions on intra-seasonal oscillations of the South Asian monsoon rainfall. *Climate Dynamics, 53*(11), 6569–6593. https://doi.org/10.1007/s00382-019-04944-5.

Singh, C., Ganguly, D., Sharma, P., & Mishra, S. (2019b). Climate response of the south Asian monsoon system to West Asia, Tibetan Plateau and local dust emissions. *Climate Dynamics, 53*(9–10), 6245–6264. https://doi.org/10.1007/s00382-019-04925-8.

Singh, C., Singh, S. K., Chauhan, P., & Budakoti, S. (2020). Simulation of an extreme dust episode using WRF-CHEM based on optimal ensemble approach. *Atmospheric Research, 249,* 105296. https://doi.org/10.1016/j.atmosres.2020.105296.

Singh, C., Thomas, L., & Kumar, K. K. (2017b). Impact of aerosols and cloud parameters on Indian summer monsoon rain at intraseasonal scale: A diagnostic study. *Theoretical and Applied Climatology, 127*(1–2), 381–392. https://doi.org/10.1007/s00704-015-1640-6.

Sokolik, I. N., Winker, D. M., Bergametti, G., Gillette, D. A., Carmichael, G., Kaufman, Y. J., et al. (2001). Introduction to special section: Outstanding problems in quantifying the radiative impacts of mineral dust. *Journal of Geophysical Research: Atmospheres, 106*(D16), 18015–18027. https://doi.org/10.1029/2000JD900498.

Su, L., & Toon, O. B. (2011). Saharan and Asian dust: similarities and differences determined by CALIPSO, AERONET, and a coupled climate-aerosol microphysical model. *Atmospheric Chemistry and Physics, 11*(7), 3263–3280. https://doi.org/10.5194/acp-11-3263-2011.

Su, L., & Fung, J. C. H. (2015). Sensitivities of WRF-Chem to dust emission schemes and land surface properties in simulating dust cycles during springtime over East Asia. *Journal of Geophysical Research: Atmospheres, 120*(21), 11215–11230. https://doi.org/10.1002/2015JD023446.

Tegen, I., & Fung, I. (1994). Modeling of mineral dust in the atmosphere: Sources, transport, and optical thickness. *Journal of Geophysical Research: Atmospheres, 99*(D11), 22897–22914. https://doi.org/10.1029/94JD01928.

Ukhov, A., Ahmadov, R., Grell, G., & Stenchikov, G. (2020). Improving dust simulations in WRF-Chem model v4.1.3 coupled with GOCART aerosol module. *Geoscientific Model Development Discussions*. https://doi.org/10.5194/gmd-2020-92.

Uno, I., Eguchi, K., Yumimoto, K., Takemura, T., Shimizu, A., Uematsu, M., et al. (2009). Asian dust transported one full circuit around the globe. *Nature Geoscience, 2*(8), 557–560. https://doi.org/10.1038/ngeo583.

Vinoj, V., Rasch, P. J., Wang, H., Yoon, J.-H., Ma, P.-L., Landu, K., & Singh, B. (2014). Short-term modulation of Indian summer monsoon rainfall by West Asian dust. *Nature Geoscience, 7*(4), 308–313. https://doi.org/10.1038/ngeo2107.

Wang, Z., Zhang, H., Jing, X., & Wei, X. (2013). Effect of non-spherical dust aerosol on its direct radiative forcing. *Atmospheric Research, 120–121,* 112–126. https://doi.org/10.1016/j.atmosres.2012.08.006.

Zeng, Y., Wang, M., Zhao, C., Chen, S., Liu, Z., Huang, X., Gao, Y. (2020). WRF-Chem v3.9 simulations of the East Asian dust storm in. (2017). modeling sensitivities to dust emission and dry deposition schemes. *Geoscientific Model Development, 13*(4), 2125–2147. https://doi.org/10.5194/gmd-13-2125-2020.

Zobler, L. (1999). Global soil types, 1-degree grid (Zobler). *ORNL DAAC*. https://doi.org/10.3334/ORNLDAAC/418.